Taylor & Francis
Taylor & Francis Group

Journal of Coordination Chemistry

ISSN: 0095-8972 (Print) 1029-0389 (Online) Journal homepage: http://www.tandfonline.com/loi/gcoo20

Structures and mesomorphism of complexes of tetrakis(4-chlorobenzoate-μ-O,O')bis(ethanol)dicopper(II) with different N-donor ligands

Norbani Abdullah, Naima Sharmin, Lailatun Nazirah Ozair, Abdul Rahman Nordin, Wan Siti Nasuha Mohd. Nasir & Mohammad Isa Mohamadin

To cite this article: Norbani Abdullah, Naima Sharmin, Lailatun Nazirah Ozair, Abdul Rahman Nordin, Wan Siti Nasuha Mohd. Nasir & Mohammad Isa Mohamadin (2015) Structures and mesomorphism of complexes of tetrakis(4-chlorobenzoate-μ-O,O')bis(ethanol)dicopper(II) with different N-donor ligands, Journal of Coordination Chemistry, 68:8, 1347-1360, DOI: 10.1080/00958972.2015.1016428

To link to this article: http://dx.doi.org/10.1080/00958972.2015.1016428

Journal of Coordination Chemistry, 2015
Vol. 68, No. 8, 1347–1360, http://dx.doi.org/10.1080/00958972.2015.1016428

Structures and mesomorphism of complexes of tetrakis (4-chlorobenzoate-μ-O,O′)bis(ethanol)dicopper(II) with different N-donor ligands

NORBANI ABDULLAH*†, NAIMA SHARMIN†, LAILATUN NAZIRAH OZAIR†, ABDUL RAHMAN NORDIN†, WAN SITI NASUHA MOHD. NASIR† and MOHAMMAD ISA MOHAMADIN‡

†Science Faculty, Chemistry Department, Universiti Malaya, Kuala Lumpur, Malaysia
‡Center of Applied Science Studies, Universiti Teknologi MARA Sarawak, Kota Samarahan, Malaysia

(*Received 11 November 2014; accepted 15 January 2015*)

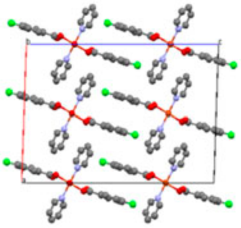

This article reports the synthesis and paddle-wheel structure of [$Cu_2(4\text{-}ClC_6H_4COO)_4(EtOH)_2$], and its reaction with pyridine (pyr), 2,2′-bipyridine (bpy), and 1,4,8,11-tetraazacyclotetradecane (cyclam) to form mononuclear covalent complexes, [$Cu(4\text{-}ClC_6H_4COO)_2(pyr)_2(H_2O)$] and [$Cu(4\text{-}ClC_6H_4COO)_2(bpy)(H_2O)$], and mononuclear ionic complex, [$Cu(cyclam)(H_2O)_2$]($4\text{-}ClC_6H_4COO)_2$, respectively. Also reported are the mesomorphic properties of [$Cu(4\text{-}ClC_6H_4COO)_2(L)_2(H_2O)$] and [$Cu(cyclam)(L)_2$]($4\text{-}ClC_6H_4COO)_2$, where L = 4-hexadecyloxypyridine. These complexes are potential molecular magnetic materials with tunable properties.

Dimeric [$Cu_2(4\text{-}ClC_6H_4COO)_4(EtOH)_2$] (**1**) reacted with pyridine (pyr), 2,2′-bipyridine (bpy), and 1,4,8,11-tetraazacyclotetradecane (cyclam) to form mononuclear covalent complexes, [$Cu(4\text{-}ClC_6H_4COO)_2(pyr)_2(H_2O)$] (**2**) and [$Cu(4\text{-}ClC_6H_4COO)_2(bpy)(H_2O)$] (**3**), and mononuclear ionic, [$Cu(cyclam)(H_2O)_2$]($4\text{-}ClC_6H_4COO)_2$ (**4**), respectively. The molecular structures of **2** and **3** were determined by single-crystal X-ray crystallography. Complexes **1** and **4** then reacted with 4-hexadecyloxypyridine (L) to form mesomorphic complexes, [$Cu(4\text{-}ClC_6H_4COO)_2(L)_2(H_2O)$] (**5**) and [Cu (cyclam)$(L)_2$]($4\text{-}ClC_6H_4COO)_2$ (**6**), respectively. These complexes are potential molecular magnetic materials with tunable properties.

Keywords: Copper(II); 4-Chlorobenzoate; Pyridine; 2,2′-Bipyridine; Cyclam; Crystal; Mesomorphism

---

*Corresponding author. Email: norbania@um.edu.my

1. Introduction

Most copper(II) carboxylates are dimeric and have paddle-wheel structures [1–16]. From EXAFS data, it was inferred that the dimers were linked into a 1-D oligomeric chain in the solid state [17], and remained intact in solutions [18, 19]. The two magnetic Cu(II) centers in the dimer are separated by 2.607 Å [20], but experience a strong antiferromagnetic interaction (2J about $-300\ \text{cm}^{-1}$ [5, 21]), postulated to occur through the bridging carboxylate ligands (the super-exchange pathway) [5]. Initial research on these complexes was focused on their potential as molecular sieve and storage, molecular magnets, and redox catalysts [22–24]. Currently, there were only a few reports on the chemical properties of these complexes, even though both Cu(II) ions are readily accessible for attacks by Lewis bases, especially N-donor ligands. The products of such reactions were either monomeric or dimeric, depending on the carboxylate and N-donor ligands involved. As examples, both monomeric [25–28] and dimeric [29–31], but only mononuclear ionic [32–36] complexes were formed in their reactions with pyridine (pyr), 2,2′-bipyridine (bpy) and 1,4,8,11-tetraazacyclotetradecane (cyclam), respectively.

Our research is focused on copper(II) carboxylates as functional molecular materials with tunable properties. We reported our findings for $[Cu_2(4\text{-}XC_6H_4COO)_4(EtOH)_2]$ (X = H [37], F [38], I [27], NO_2 [28]), and $[Cu_2(R)_4(RH)_2]$ (R = 2-hexyldecanoate ion) [14]. This article reports: (a) the synthesis, spectral, electrochemical, and thermal studies of $[Cu_2(4\text{-}ClC_6H_4COO)_4(EtOH)_2]$ (**1**) in order to establish its dimeric paddle-wheel structure; (b) reactions of **1** with pyr, bpy, and cyclam to form $[Cu(4\text{-}ClC_6H_4COO)_2(pyr)_2(H_2O)]$ (**2**), $[Cu(4\text{-}ClC_6H_4COO)_2(bpy)(H_2O)]$ (**3**), $[Cu(cyclam)(H_2O)_2](4\text{-}ClC_6H_4COO)_2$ (**4**), respectively; and (c) reactions of **1** and **4** with 4-hexadecyloxypyridine (L) to form $[Cu(4\text{-}ClC_6H_4COO)_2(L)_2(H_2O)]$ (**5**) and $[Cu(cyclam)(L)_2](4\text{-}ClC_6H_4COO)_2$ (**6**), respectively. These reactions are shown in scheme 1. Complexes **2–6** were mononuclear, **2** and **3** were single crystals, **4** was ionic, and **5** and **6** were mesomorphic. We infer from our results that

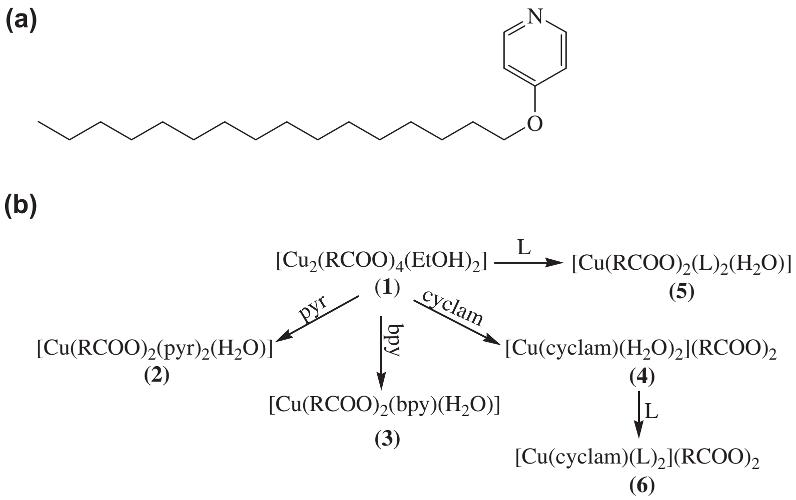

Scheme 1. (a) Structural formula of 4-hexadecyloxypyridine (L); (b) syntheses of **2–6** (R = $4\text{-}ClC_6H_4$; L = 4-hexadecyloxypyridine).

the dimeric structure of **1** dissociated to monomers, which then reassembled with the N-donor ligand present. Hence, these reactions may serve as facile routes for the formation of covalent and ionic magnetic complexes.

2. Experimental

2.1. *Materials and measurements*

All chemicals were commercially available and used as received. ^{1}H NMR spectrum was recorded on a JEOL FT-NMR lambda 400-MHz spectrometer. Elemental analyses were recorded on a Thermo Finnigan Flash EA 110 CHNS/O analyzer, and the copper content was determined on a PerkinElmer Analyst 800 flame atomic absorption spectrometer. FTIR spectra were recorded from 4000 to 450 cm^{-1} on a Perkin-Elmer Frontier FTIR spectrophotometer equipped with a diamond attenuated total reflectance attachment. Electronic absorption and reflectance spectra were recorded on a Shimadzu UV–vis-NIR 3600 spectrophotometer. Magnetic susceptibilities were measured at room temperature on a Sherwood automagnetic susceptibility balance by the Gouy method, using $Hg[Co(NCS)_4]$ as the calibrant. Powder X-ray diffractography (PXRD) was recorded at room temperature on a Siemens D5000 X-ray diffractometer, using Cu-Kα (λ = 1.54056 Å) radiation as the X-ray source. The scattering angle was 2–80°, applied voltage was 40 kV, and current was 40 mA. Thermogravimetric analysis (TGA) was carried out on a Perkin-Elmer TGA 6 in the temperature range 30–900 °C under N_2 at a flow rate of 10 cm^3 min^{-1} and scan rate of 20 °C min^{-1}. Cyclic voltammetry (CV) was run on a Gamry Instrument Reference 600 potentiostat/galvanostat/ZRA; the voltage range was from −1.5 V to +1.5 V, and scan rate was 100 mV s^{-1}. A three-electrode cell consisting of a glassy carbon as the working electrode, a saturated calomel electrode as the reference electrode, and a platinum wire as the counter electrode was used. The supporting electrolyte was tetra-*n*-butylammonium tetrafluoroborate (TBATFB), and the molarities of the electrolyte and sample in $CH_3OH–CH_3COOH$ (20 : 1 v/v) were 0.1 and 0.0015 M, respectively. The solutions were bubbled with N_2 prior to measurements. Differential scanning calorimetry (DSC) was carried out on a Mettler Toledo DSC 822 instrument from 25 to 150 °C under N_2 at a flow rate of 20 cm^3 min^{-1} and scan rate of 10 °C min^{-1}. The onset temperatures were quoted for all peaks observed. Polarizing optical microscopy (POM) was carried out on an Olympus polarizing microscope equipped with a Mettler Toledo FP90 central processor and a Linkam THMS 600 hot stage. The heating and cooling rates were 10 and 2 °C min^{-1}, respectively, and the magnification was 50×.

2.2. *Synthesis of 4-hexadecyloxypyridine (L)*

1-Bromohexadecane (50.8 mmol, 15.25 g) was added portion wise to a vigorously stirred mixture of 4-hydroxypyridine (52.7 mmol, 5.01 g), K_2CO_3 (125.2 mmol, 17.28 g), and KI (2.0 mmol, 0.33 g) in DMF (200 cm^3) at room temperature. The mixture was refluxed for 24 h, cooled to room temperature, and poured into distilled water. The pale yellow solid obtained was washed several times with distilled water, purified using hot ethanol, and dried in an oven at 60 °C. Yield: 88.8%. IR (neat, cm^{-1}): 2920 (s), 2850 (s), 1638 (s), 1596 (s), 1188 (s). ^{1}H NMR (400 MHz, $CDCl_3$): $\delta = 0.88$ (t, 3H, CH_3), 1.25 (m, 28H, $–OCH_2(\mathbf{CH_2})_{14}$, 3.75 (t, 2H, $–O\mathbf{CH_2}(CH_2)_{14}$, 6.39 (q, $2H_{aromatic}$), 7.26 (m, $2H_{aromatic}$) ppm.

2.3. *Synthesis of [$Cu_2(4\text{-}ClC_6H_4COO)_4(EtOH)_2$] (1)*

Copper(II) acetate monohydrate (20.0 mmol, 4.00 g) was added portion wise to a magnetically stirred hot ethanolic solution (95%, 50 cm^3) of 4-chlorobenzoic acid (40.0 mmol, 6.26 g). The mixture was further heated for an hour, and the greenish-blue powder obtained was filtered from the hot solution, washed several times with hot ethanol, and dried in an oven at 90 °C. Yield: 48.0%. Anal. Calcd for $C_{16}H_{14}Cl_2CuO_5$: C, 45.7; H, 3.3; Cu, 15.1. Found: C, 45.8; H, 3.3; Cu, 15.6. IR (neat, cm^{-1}): 3400 (br), 1600 (vs), 1408 (vs), 840 (s), 600 (s).

2.4. *Synthesis of [$Cu(4\text{-}ClC_6H_4COO)_2(pyr)_2(H_2O)$] (2)*

A few drops of pyridine were added to an ethanolic suspension of **1** (0.42 mmol, 0.35 g) at room temperature until a purple solution formed. The solution was gently heated for 30 min and filtered while still hot. Dark-blue crystals deposited from the filtrate after one week at room temperature. Yield: 82.6%.

2.5. *Synthesis of [$Cu(4\text{-}ClC_6H_4COO)_2(bpy)(H_2O)$] (3)*

2,2′-Bipyridine (0.77 mmol, 0.12 g) was added to an ethanolic suspension of **1** (0.29 mmol, 0.24 g). The mixture was heated for 30 min, and the dark-blue solution formed was filtered while still hot. Dark-blue crystals deposited from the filtrate after one week at room temperature. Yield: 75.0%.

2.6. *Synthesis of [$Cu(cyclam)(H_2O)_2$]($4\text{-}ClC_6H_4COO)_2$ (4)*

An ethanolic solution of cyclam (0.50 mmol, 0.10 g) was added portion wise to a hot ethanolic suspension of **1** (0.83 mmol, 0.70 g). The purple solution formed was heated for 30 min and filtered while still hot. Dark-purple powder deposited at room temperature. Yield: 80.6%. Anal. Calcd for $C_{24}H_{36}Cl_2CuN_4O_6$: C, 47.18; H, 5.94; N, 9.17. Found: C, 47.03; H, 5.96; N, 9.01. IR (neat, cm^{-1}): 3146 (br), 2919 (w), 1739 (w), 1658 (m), 1592 (s), 1547 (s), 1371 (vs), 779 (s), 522 (vs).

2.7. *Synthesis of [$Cu(4\text{-}ClC_6H_4COO)_2(L)_2(H_2O)$] (5)*

A solution of **1** (0.76 mmol, 0.64 g) and L (1.6 mmol, 0.50 g) in a mixture of ethanol (95%, 100 cm^3) and DMSO (99%, 50 cm^3) was gently heated for one hour and filtered while still hot. The blue powder formed from the filtrate on cooling was washed several times with ethanol and dried in an oven at 60 °C. Yield: 38.9%. Anal. Calcd for $C_{56}H_{84}Cl_2CuN_2O_7$: C, 65.19; H, 8.21; N, 2.72. Found: C, 64.86; H, 8.34; N, 2.54. IR (neat, cm^{-1}): 3600 (w), 2916 (m), 2850 (m), 1741 (m), 1658 (m), 1587 (s), 1397 (s), 1380 (s), 1342 (vs), 920 (s), 870 (s), 569 (s).

2.8. *Synthesis of [$Cu(cyclam)(L)_2$]($4\text{-}ClC_6H_4COO)_2$ (6)*

An ethanolic solution of **4** (0.61 mmol, 0.37 g) and L (1.2 mmol, 0.37 g) was gently heated for 10 min, filtered while still hot, and left to cool to room temperature. The product was a dark-purple powder. Yield: 60.0%. Anal. Calcd for $C_{66}H_{106}Cl_2CuN_6O_6$: C, 65.30; H, 8.80; N, 6.92. Found: C, 65.13; H, 8.95; N, 6.67. IR (neat, cm^{-1}): 3360 (br), 2918 (vs), 2850 (s), 1637 (m), 1592 (s), 1536 (vs), 1468 (m), 1381 (vs), 1188 (m), 1092 (m), 1010 (m), 858 (m), 777 (m), 521 (s).

2.9. *Crystallographic data collection and structural determination*

Single-crystal X-ray diffraction data were collected on a Bruker SMART APEX II CCD fitted with Mo-Kα radiation, so that θ_{max} was 27.5°. The data-set was corrected for absorption based on multiple scans [39] and reduced using standard methods [40]. The structures were solved by direct methods with SHELXS97 [41], and refined by a full-matrix least-squares procedure on F^2 using SHELXL97 with anisotropic displacement parameters for non-hydrogen atoms and a weighting scheme of the form $w = 1/[\sigma^2(F_o^2) + aP^2 + bP]$, where $P = (F_o^2 + 2F_c^2)/3)$. All hydrogens were included in the final refinement in their calculated positions. The crystallographic data and selected bond lengths and angles for **1** and **2** are listed in tables 1 and 2. Crystallographic data for the structural analyses have been deposited at the Cambridge Crystallographic Data Center.

Table 1. Crystal data and structure refinement for **2** and **3**.

Complex	**2**	**3**
Chemical formula	$C_{24}H_{20}Cl_2CuN_2O_5$	$C_{24}H_{18}Cl_2CuN_2O_5$
Formula mass (g mol^{-1})	550.88	548.84
T (K)	293(2)s	293(2)
λ (Å)	0.71073	0.71073
Crystal system	Monoclinic	Triclinic
Space group	*C2/c*	*P-1*
a (Å)	15.914(3)	8.0436(8)
b (Å)	6.0705(10)	9.8446(9)
c (Å)	23.673(4)	15.133(14)
α (°)	90	78.8440(10)
β (°)	92.072(3)	81.6400(10)
γ (°)	90	71.2980(10)
V ($Å^3$)	2285.5(7)	1109.14(18)
Z	4	2
D_{calc} (g cm^{-3})	1.595	1.589
Absorption coefficient (mm^{-1})	1.230	1.261
F(0 0 0)	1116	538
θ range (°)	2.56–25.00	1.38–25.00
Index ranges	$-18 \le h \le 18$ $-7 \le k \le 7$ $-28 \le l \le 28$	$-9 \le h \le 9$ $-11 \le k \le 11$ $-17 \le l \le 17$
Reflections collected	11,525	11,627
Independent reflections (R_{int})	2009 (0.0682)	3912 (0.0466)
Data/restraints/parameters	2009/0/155	3912/0/311
Goodness-of-fit on F^2	1.490	0.845
Final R indices [$I \ge 2.0\ \sigma(I)$]	$R_1 = 0.0724$ $wR_2 = 0.2016$	$R_1 = 0.0342$ $wR_2 = 0.0981$
R indices (all data)	$R_1 = 0.0907$ $wR_2 = 0.2164$	$R_1 = 0.0517$ $wR_2 = 0.1216$
$\Delta\rho_{max}$, $\Delta\rho_{min}$ (e $Å^{-3}$)	0.625, −1.401	0.455, −0.521

Table 2. Selected bond lengths (Å) and angles (°) for **2** and **3**.

	2	**3**
Bond length		
Cu(1)–O(1)	1.943(4)	1.954(2)
Cu(1)–O(2)	1.943(4)	1.982(2)
Cu(1)–N(1)	2.015(5)	1.997(3)
Cu(1)–N(2)	2.015(5)	2.010(3)
Angle		
O(1)–Cu(1)–O(2)	178.2(2)	95.11(9)
O(1)–Cu(1)–N(1)	89.49(18)	91.00(10)
O(1)–Cu(1)–N(1)	90.70(18)	166.50(10)
O(1)–Cu(1)–N(2)	90.70(18)	169.06(10)
O(2)–Cu(1)–N(2)	89.49(18)	91.23(10)
N(1)–Cu(1)–N(2)	167.5(3)	81.00(11)
O(1)–Cu(1)–O(1W)	89.12(12)	97.02(9)
O(2)–Cu(1)–O(1W)	89.12(12)	90.33(9)
N(1)–Cu(1)–O(1W)	96.25(13)	100.87(10)
N(2)–Cu(1)–O(1W)	96.25(13)	91.83(10)

3. Results and discussion

3.1. *Synthesis and structural deduction of complex 1*

The synthetic method to obtain a dimeric copper(II) arylcarboxylate adopting the paddle-wheel structure involves a metathesis reaction between [$Cu_2(CH_3COO)_4(H_2O)_2$] and an arylcarboxylic acid (mole ratio = 1 : 2) [42]. By this method, we obtained [Cu_2(4-$ClC_6H_4COO)_4(EtOH)_2$] (**1**) as a greenish-blue powder in 48.0% yield. Its chemical formula and paddle-wheel structure were supported by elemental analyses (Experimental) and by comparing its other data with those obtained for crystals of copper(II) carboxylates exhibiting this structure (table 3).

The IR spectrum of **1** showed a broad peak at 3400 cm^{-1} for $\bar{v}$OH, a strong peak at 1562 cm^{-1} for $\bar{v}_{asym}$COO, and a strong peak at 1408 cm^{-1} for $\bar{v}_{sym}$COO. The difference (Δ) in the latter two peaks was 154 cm^{-1}. Its electronic spectra showed broad *d–d* bands at 703 and 300 nm for a solid sample, and at 700 nm (ε_{max} = 283 M^{-1} cm^{-1}) and 380 nm (ε_{max} = 66 M^{-1} cm^{-1}) for a solution in CH_3OH–CH_3COOH (20 : 1 v/v). These data suggest

Table 3. Data for **1** and other paddle-wheel crystalline complexes.

Complex	Δ[a] (cm^{-1})	λ/nm (ε_{max}/M^{-1} cm^{-1})	μ_{eff} (BM)	Ref.
[$Cu_2(4\text{-}ClC_6H_4COO)_4(EtOH)_2$]	154	703[b]; 700 (283)[c]	1.8	This work
[$Cu_2(R1)_4(EtOH)_2$]	144	694[b]	na	[7]
[$Cu_2(HCOO)_4(dmf)_2$]	169	719[b]	1.6	[9]
[$Cu_2(R2)_4(H_2O)_2$].3dmf	206	704, 385[b]	2.1	[10]
[$Cu_2(R3)_4(MeCN)_2$]	198	698, 380[b]	na	[12]
[$Cu_2(R4)_4(pyr)_2$]	200	na	na	[13]
[$Cu_2(CH_3(CH_2)_5COO)_4$]	173	671 (375)[c]	1.6	[14]
[$Cu_2(CH_3COO)_4(tnz)_2$]	199	713 (210)[c]	1.3	[15]

Notes: na = not available; R = 1-phenylcyclopropane-1-carboxylato; R2 = 2,6-$(MeO)_2$nicotinate; R3 = 2-$O_2NC_6H_4COO$; R4 = 4-$ClC_6H_4CH_2COO$; tnz = tinidazole.
[a] Δ = $\bar{v}_{asym}$COO − $\bar{v}_{sym}$COO.
[b] Reflectance.
[c] Absorbance.

a square pyramidal geometry [43] at both Cu(II) centers in the solid form and in these solvents. Since these data were similar to crystals of copper(II) complexes with the dimeric paddle-wheel structures reported in the literature [12–15] (table 3), we inferred that **1** also has this structure.

The effective magnetic moment (μ_{eff}) for **1** was 1.8 BM at 300 K. The value was determined by the Gouy method, and calculated for the dimer using the equation: $\mu_{\text{eff}} = 2.83\left[\left(\chi_{\text{M}}^{\text{corr}} - \text{N}\alpha\right)T\right]^{1/2}$, where $\chi_{\text{M}}^{\text{corr}}$ (1.43×10^{-3} cm^3 mol^{-1}) was the molar magnetic susceptibility corrected for the diamagnetic contribution of the constituent atoms estimated from Pascal's constant [44], T was the absolute temperature, and Nα was the temperature-independent paramagnetism (60×10^{-6} cm^3 mol^{-1} per Cu(II) [45]. The experimental μ_{eff} value was significantly lower than the expected spin-only value (2.45 BM) for a dinuclear Cu(II) complex ($\chi_{\text{M}}^{\text{corr}}T = 0.375$ per Cu(II) for $g = 2.0$ [46]). This suggested a strong antiferromagnetic interaction between the Cu(II) ions in this complex. The value was also higher than reported for [$Cu_2(CH_3(CH_2)_5COO)_4$] (1.6 BM) [14] and [$Cu_2(CH_3COO)_4(tnz)_2$] (tnz = tinidazole; 1.3 BM) [15], suggesting a weaker antiferromagnetic interaction between the two Cu(II) atoms in **1**. We ascribed this to the differences in the electronic effect of the group bonded to –COO of the carboxylate and the type of donor atom of the apical ligand (N-donors are stronger Lewis bases than O-donors). This is based on the conclusion made by Yamanaka *et al.* that a higher charge density on the carboxylate carbon resulted in a stronger antiferromagnetic interaction in copper(II) carboxylates [5].

PXRD was done for **1** in an attempt to correlate magnetism with crystallinity, interplanar distance (d), and particle size (D). The diffractogram (figure 1) indicates that the complex was polycrystalline, and the values for d and D were 11.042 and 13.873 Å, respectively. These values were calculated from its most intense peak ($2\theta = 8°$) using the Bragg ($2d \sin \theta = n\lambda$) and Scherrer ($D = 0.99\ \lambda/(\beta_{½} \cos \theta)$, where $\beta_{½}$ = full width at half maximum of the Bragg peak) equations, respectively. Hence, compared with [$Cu_2(C_6H_5COO)_4(EtOH)_2$] ($d$ = 16.819 Å; D = 8.981 Å; μ_{eff} = 1.9 BM) [37] and [$Cu_2(4\text{-}FC_6H_4COO)_4(EtOH)_2$] ($d$ = 15.768 Å; D = 10.907 Å; μ_{eff} = 2.5 BM) [38], complex **1** has a shorter interplanar distance and larger particle size. These parameters seem to account for the stronger antiferromagnetic interaction between the two Cu(II) centers in **1**.

TGA for **1** was done to check its purity and thermal stability. The trace shows an initial weight loss of 10.9% from 87 to 170 °C due to loss of the axially coordinated EtOH molecules (Calcd 11.0%). The complex then lost 72.3% from 288 to 700 °C due to decarboxylation of 4-ClC_6H_4COO ligand (Calcd 74.0%). The amount of residue above 700 °C was

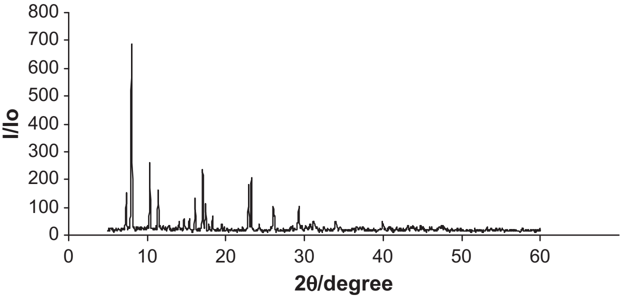

Figure 1. PXRD of [$Cu_2(4\text{-}ClC_6H_4COO)_4(EtOH)_2$].

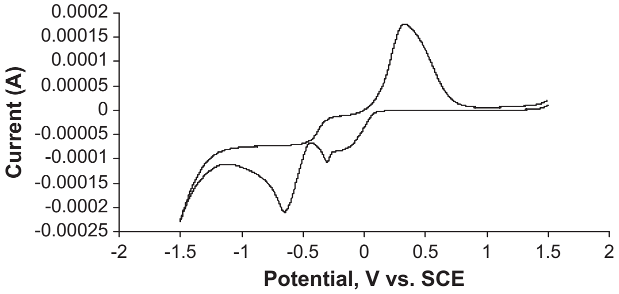

Figure 2. Cyclic voltammogram of **1** in CH_3OH-CH_3COOH (20 : 1 v/v).

16.8%, which was in agreement with the value calculated from its chemical formula (18.9%), assuming pure CuO [47]. **1** ($T_{dec} = 288$ °C) was more thermally stable than $[Cu_2(C_6H_5COO)_4(EtOH)_2]$ ($T_{dec} = 254$ °C) [37] and $[Cu_2(4\text{-}FC_6H_4COO)_4(EtOH)_2]$ ($T_{dec} = 275$ °C) [38]. Since the initial step in the thermal decomposition of these complexes involves loss of CO_2 from the carboxylate [37], it is inferred that for **1**, the 4-ClC_6H_4–COO^- bond was stronger than C_6H_5–COO^- and 4-FC_6H_4–COO^- bonds. This is consistent with the electronic effect of Cl suggested above.

Finally, CV was carried out for **1** in order to probe its nuclearity and structural stability in CH_3OH-CH_3COOH (20 : 1 v/v). The scan (figure 2) shows three reduction peaks at $E_{pc} = -0.19$ V, -0.32 V, and -0.68 V, and a broad oxidation peak at $E_{pa} = +0.37$ V, against Ag/AgCl, saturated KCl. The peak separations (560–1050 mV) far exceeded the theoretical value for a reversible one-electron redox process (56 mV at 298 K [48]), indicating quasireversible redox processes and hence extensive structural changes. These results were similar to $[Cu_2(C_6H_5COO)_4(EtOH)_2]$ ($E_{pc} = -0.13$ V, -0.35 V, and -0.74 V; $E_{pa} = +0.31$ V, $+0.46$ V) [37], but quite different from $[Cu_2(4\text{-}ClC_6H_4CH_2COO)_4(pyr)_2]$ ($E_{pc} = -0.61$ V; $E_{pa} = +0.66$ V) [13] and $[Cu_2(CH_3COO)_4(tnz)_2]$ ($E_{pc} = -0.12$ V; $E_{pa} = +0.20$ V) [15]. From these, we infer that the dimers partially dissociated to monomers in these solvents prior to the redox process(es) (scheme 2). This is based on the fact that copper(II) complexes are labile in solutions, and the equatorial Cu–O bonds are weakened when the apical positions are coordinated by EtOH (O-donor ligand). Similar chemical–electrochemical–chemical mechanism (CEC) was suggested for $[Cu_2(C_6H_5COO)_4(EtOH)_2]$ [37]. Hence, the CV results support the dimeric structure for **1,** and account for the mononuclear complexes obtained from the reaction of **1** with the N-donor ligands (stronger Lewis bases than O-donor ligands), discussed below.

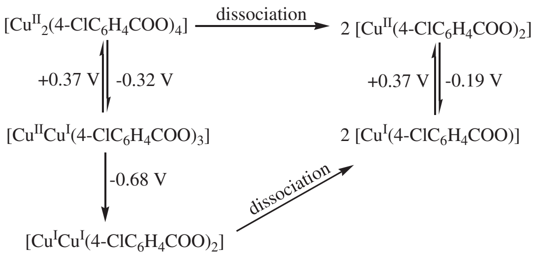

Scheme 2. The CEC for **1**.

3.2. *Reaction of 1 with N-donor and N_2-donor ligands*

Complex **1** reacted with pyr and with bpy to form mononuclear complexes, [Cu(4-$ClC_6H_4COO)_2$(pyr)$_2$(H_2O)] (**2**) and [Cu(4-$ClC_6H_4COO)_2$(bpy)(H_2O)] (**3**), respectively. Both complexes were dark-blue single crystals. The crystallographic and structure refinement data for both crystals are given in table 1, while selected bond lengths and angles are given in table 2.

Complex **2** crystallized in the monoclinic crystal system with *C2*/c space group. Its molecular structure (figure 3) shows mononuclear units, with each Cu(II) coordinated by two monodentate 4-$ClC_6H_4COO^-$ and two monodentate pyridines at the basal plane, and a H_2O at the apical site. Both organic ligands were *trans* to each other. The bond distances

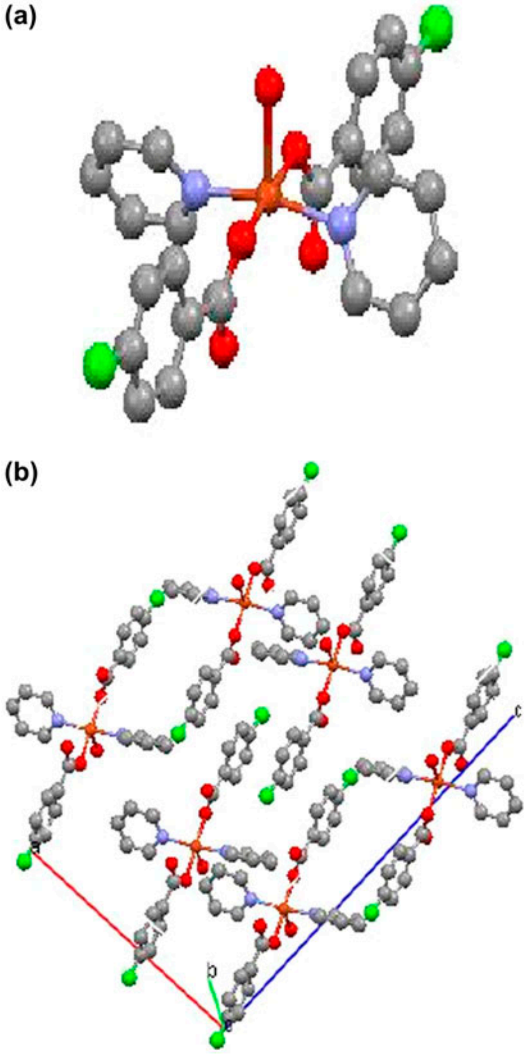

Figure 3. (a) ORTEP view and (b) packing diagram of **2** at 30% thermal ellipsoids. The hydrogens were removed for clarity.

and angles indicate a distorted square pyramidal geometry (CuN_2O_3 chromophore), with the Cu(II) out of the basal plane toward the apex of the pyramid by 0.030 Å. The two non-coordinated oxygens from each carboxylate were not coordinated to Cu(II), but instead formed H-bonds (2.770 Å) with the axially coordinated H_2O ligand from a neighboring molecule, forming a 1-D structure. **2** has a similar structure to $[Cu(C_6H_5COO)_2(H_2O)(pyr)_2]$ [25], but different from $[Cu(4\text{-}HOC_6H_4COO)_2(pyr)_2]$ [26] and $[Cu_2(4\text{-}ClC_6H_4CH_2COO)_4(pyr)_2]$ [13].

Complex **3** crystallized in the triclinic crystal system with *P-1* space group. Its molecular structure (figure 4) shows mononuclear units with square pyramidal Cu(II). However, its molecular structure was quite different from **2**. At the basal plane were a chelating bpy, a monodentate $4\text{-}ClC_6H_4COO^-$ and H_2O, while at the apex was a monodentate $4\text{-}ClC_6H_4COO^-$ ligand. The oxygen of the basal and apical $4\text{-}ClC_6H_4COO^-$ was intramolecularly H-bonded

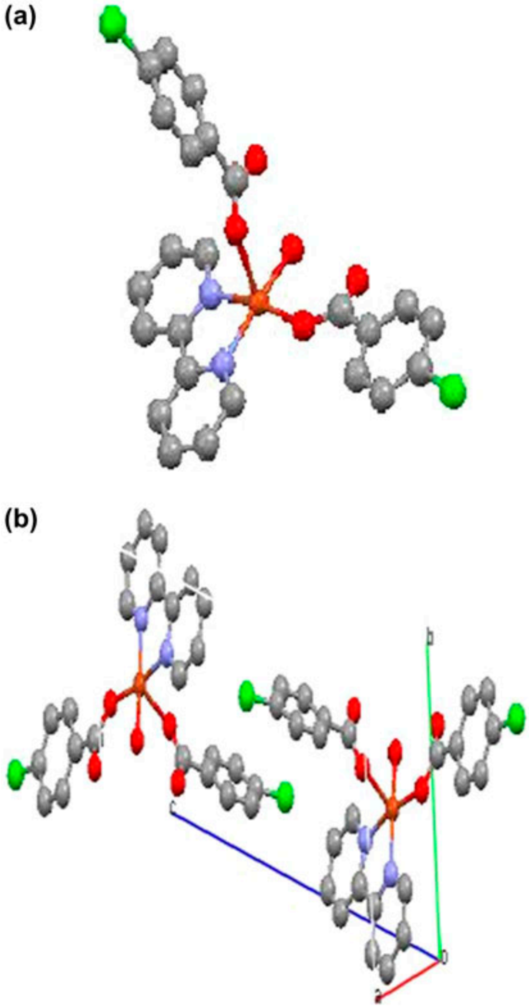

Figure 4. (a) ORTEP view and (b) packing diagram of **3** at 30% thermal ellipsoids. The hydrogens were removed for clarity.

to H_2O (1.631 Å). Its molecular structure was also different from $[Cu(4\text{-}IC_6H_4COO)_2(bpy)(H_2O)]$ [27], $[Cu_2(C_6H_5COO)_4(bpy)_2]$ [30] and $[Cu(3,5\text{-}NO_2)_2C_6H_3COO)_2(H_2O)(bpy)]$ [31].

3.3. *Reaction of 1 with cyclam*

Complex **1** reacted with cyclam, a N_4-donor macrocycle, to form a dark-purple powder in good yield (80.6%). Its structural formula, $[Cu(cyclam)(H_2O)_2](4\text{-}ClC_6H_4COO)_2$ (**4**), was proposed based on the results of elemental analyses (Experimental) and spectral data comparison with crystals of similar complexes [34–36] (table 4). Hence, compared with mononuclear covalent **2** and **3**, complex **4** was mononuclear and ionic.

3.4. *Mesomorphic complexes*

Both **1** and **4** have O-donor ligands (EtOH and H_2O, respectively) at the apical positions, which may be readily replaced by a stronger N-donor ligand. Therefore, we reacted these complexes with 4-hexadecyloxypyridine (L), a pyridine derivative with a linear 16-carbon alkyl chain, in order to form magnetic mesomorphic complexes. The products were $[Cu(4\text{-}ClC_6H_4COO)_2(L)_2(H_2O)]$ (**5**) and $[Cu(cyclam)(L)_2](4\text{-}ClC_6H_4COO)_2$ (**6**), respectively. Comparing their IR and UV–vis spectral data (tables 1 and 4), it is proposed that **5** has similar structure as **2**, while **6** has similar structure as **4**.

The mesomorphisms of L, **5,** and **6** were studied by DSC and POM. From both techniques, the melting and clearing temperatures and the corresponding enthalpy changes for

Table 4. IR and UV–vis spectral data for **4–6** and similar complexes.

Complex	IR Δ (cm^{-1})	UV–vis λ_{max} (nm) [ε_{max} (M^{-1} cm^{-1})]
$[Cu(cyclam)(H_2O)_2](4\text{-}ClC_6H_4COO)_2$ (**4**)	176	541 (87)
$[Cu(4\text{-}ClC_6H_4COO)_2(L)_2(H_2O)_2]$ (**5**)	190	713 (84)
$[Cu(cyclam)(L)_2](4\text{-}ClC_6H_4COO)_2$ (**6**)	155	541 (45)
$[Cu(cyclam)(H_2O)_2](C_6H_5COO)_2\cdot 2H_2O$ [34]	162	503 (83)
$[Cu(cyclam)(H_2O)_2](4\text{-}CH_3C_6H_4COO)_2\cdot H_2O$ [35]	145	531 (105)
$[Cu(cyclam)(H_2O)_2](C_6F_5COO)_2\cdot 2H_2O$ [36]	154	522 (105)

$$\mathrm{L} \xrightarrow[14.1\ \mathrm{kJ\ mol^{-1}}]{42.9\ ^{o}\mathrm{C}} \mathrm{M} \xrightarrow[2.1\ \mathrm{kJ\ mol^{-1}}]{51.9\ ^{o}\mathrm{C}} \mathrm{I}$$

$$\mathbf{5} \xrightarrow[31.5\ \mathrm{kJ\ mol^{-1}}]{128.1\ ^{o}\mathrm{C}} \mathrm{M} \xrightarrow{155\ ^{o}\mathrm{C}} \mathrm{I}$$

$$\mathbf{6} \xrightarrow[165.0\ \mathrm{kJ\ mol^{-1}}]{70.0\ ^{o}\mathrm{C}} \mathrm{M} \xrightarrow{127\ ^{o}\mathrm{C}} \mathrm{I}$$

Scheme 3. Phase transition temperatures and enthalpy changes for L, **5,** and **6** (M = mesophase, I = isotropic liquid).

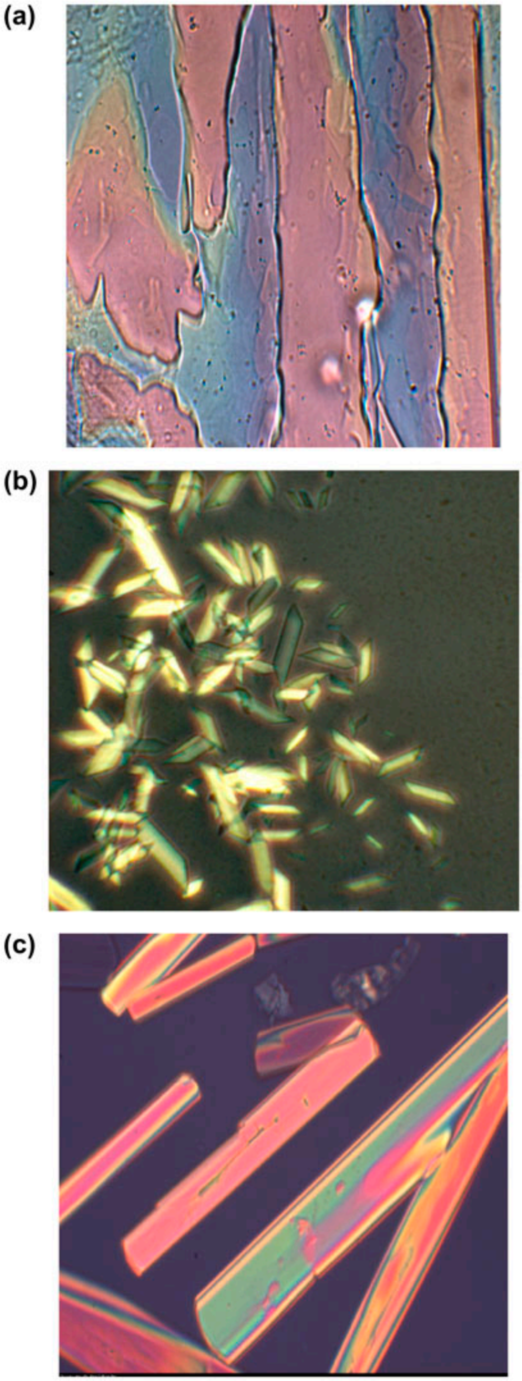

Figure 5. Photomicrographs of: (a) L at 49.0 °C; (b) **5** at 141.2 °C; and (c) **6** at 100.0 °C, on cooling from the respective isotropic liquid.

these compounds are shown in scheme 3. Their optical textures, recorded on cooling from their respective isotropic liquid, are shown in figure 5. Hence, the melting temperatures of L, **5,** and **6** were 42.9, 128.1, and 70.0 °C, respectively. They also exhibited mesomorphisms L was smectogenic, while **5** and **6** were discotic. The optical textures of **5** and **6** were quite similar, from which we imply that both complexes have similar shapes.

4. Conclusion

We presented instrumental and literature data to support the dimeric paddle-wheel structure for $[Cu_2(4\text{-}ClC_6H_4COO)_4(EtOH)_2]$ (**1**). Complex **1** reacted with pyr and bpy to form mononuclear covalent crystalline complexes, $[Cu(4\text{-}ClC_6H_4COO)_2(pyr)_2(H_2O)]$ (**2**) and $[Cu(4\text{-}ClC_6H_4COO)_2(bpy)(H_2O)]$ (**3**), respectively. However, the molecular structure of **2** showed two monodentate $4\text{-}ClC_6H_4COO^-$ and two pyridines at the basal plane, and a H_2O at the apex, while **3** showed one monodentate $4\text{-}ClC_6H_4COO$, bpy and H_2O at the basal plane, and one monodentate $4\text{-}ClC_6H_4COO^-$ at the apex. In contrast, **1** reacted with cyclam to form a mononuclear ionic complex, $[Cu(cyclam)(H_2O)_2](4\text{-}ClC_6H_4COO)_2$ (**4**). Finally, **1** and **4** reacted with 4-hexadecyloxypyridine (L) to form $[Cu(4\text{-}ClC_6H_4COO)_2(L)_2(H_2O)]$ (**5**) and $[Cu(cyclam)(L)_2](4\text{-}ClC_6H_4COO)_2$ (**6**), respectively. By comparing their analytical data, we inferred that **4** has similar structure as crystalline complexes formed from the reaction of $[Cu_2(RCOO)_4]$ ($R = C_6H_5$, $4\text{-}CH_3C_6H_4$, C_6F_5) with cyclam, **5** has similar structure to **2**, and **6** has similar to **4**. L, **5,** and **6** have low melting temperatures and exhibited mesomorphisms. Hence, all of these complexes were potential molecular magnetic materials with tunable properties.

Supplementary material

CCDC-1024683 (complex **2**) and 1025701 (complex **3**) contain the supplementary crystallographic data for this article. These data can be obtained free of charge from the Cambridge Crystallographic Data Center via www.ccdc.cam.ac.uk/data_request/cif.

Funding

This work was supported by the Malaysia Ministry of Education for High Impact Research [grant number UM.C/625/1/HIR/MOHE/05], Fundamental Research Grant Scheme [grant number FP031-2013B], and Universiti Malaya for Postgraduate Research [grant number PV056-2012A], [grant number PG023-2013A].

References

[1] W. Harrison, S. Retig, J. Trotter. *J. Chem. Soc., Dalton Trans.*, 1852 (1972).
[2] M. Melník, M. Dunaj Jurčo, M. Handlovič. *Inorg. Chim. Acta*, **86**, 185 (1984).
[3] L.S. Erre, G. Micera, P. Piu, F. Cariati, G. Ciani. *Inorg. Chem.*, **24**, 2297 (1985).
[4] G.C. Campbell, J.F. Haw. *Inorg. Chem.*, **27**, 3706 (1988).
[5] M. Yamanaka, H. Uekusa, S. Ohba, Y. Saito, S. Iwata, M. Kato, T. Tokii, Y. Muto, O. Steward. *Acta Crystallogr., Sect. B: Struct. Sci.*, **47**, 344 (1991).
[6] T. Kawata, H. Uekusa, S. Ohba, T. Furukawa, T. Tokii, Y. Muto, M. Kato. *Acta Crystallogr., Sect. B: Struct. Sci.*, **48**, 253 (1992).

[7] F.P.W. Agterberg, H.A.J.P. Kluit, W.L. Driessen, H. Oevering, W. Buijs, M.T. Lakin, A.L. Spek, J. Reedijk. *Inorg. Chem.*, **36**, 4321 (1997).

[8] A. Elmali. *Turk. J. Phys.*, **24**, 667 (2000).

[9] R. Cejudo, G. Alzuet, J. Borrás, M. Liu-González, F. Sanz-Ruiz. *Polyhedron*, **21**, 1057 (2002).

[10] J. Jašková, D. Mikloš, M. Korabik, V. Jorík, P. Segl'a, B. Kaliňaková, D. Hudecová, J. Švorec, A. Fischer, J. Mrozinski, T. Lis, M. Melník. *Inorg. Chim. Acta*, **360**, 2711 (2007).

[11] J. Moncol, M. Mudra, P. Lönnecke, M. Hewitt, M. Valko, H. Morris, J. Svorec, M. Melnik, M. Mazur, M. Koman. *Inorg. Chim. Acta*, **360**, 3213 (2007).

[12] C.-S. Liu, J.-J. Wang, L.-F. Yan, Z. Chang, X.-H. Bu, E. C. Sañudo, J. Riba. *Inorg. Chem.*, **46**, 6299 (2007).

[13] J. Moncol, Z. Vasková, P. Stachová, J. Svorec, R. Sillanpää, M. Mazúr, D. Valigura. *J. Chem. Crystallogr.*, **40**, 179 (2010).

[14] M. Iqbal, I. Ahmad, S. Ali, N. Muhammad, S. Ahmed, M. Sohail. *Polyhedron*, **50**, 524 (2013).

[15] N. Abdullah, Y. Al-Hakem, N. Abdullah, H. Samsudin, N.S. Ahmad Tajidi. *Asian J. Chem.*, **26**, 987 (2014).

[16] R.C. Santra, K. Sengupta, R. Dey, T. Shireen, P. Das, P.S. Guin, K. Mukhopadhyay, S. Das. *J. Coord. Chem.*, **67**, 265 (2014).

[17] D. Guillon, A. Skoulios. *J. Phys. IV*, **C4**, 41 (1996).

[18] M. Kondo, M. Kubo. *J. Phys. Chem.*, **62**, 468 (1958).

[19] J.F. Boas, J.R. Pilbrow, T.D. Smith. *J. Chem. Soc.*, **A**, 721 (1969).

[20] J.N. van Niekerk, F.R.L. Schoening. *Acta Cryst.*, **6**, 227 (1953).

[21] M. Kato, Y. Muto. *Inorg. Chem. Rev.*, **92**, 45 (1988).

[22] O.M. Yaghi, H. Li, C. Davis, D. Richardson, T.L. Groy. *Acc. Chem. Res.*, **31**, 474 (1998).

[23] A.J. Blake, N.R. Champness, P. Hubberstey, W.-S. Li, M.A. Withersby, M. Schröder. *Coord. Chem. Rev.*, **183**, 117 (1999).

[24] B. Moulton, M. Zaworotko. *Chem. Rev.*, **101**, 1629 (2001).

[25] T. Ohmura, W. Mori, T. Takei, T. Ikeda, A. Maeda. *Mater. Sci.-WROCLAW-*, **23**, 729 (2005).

[26] L.N. Ozair, N. Abdullah, K.M. Lo. *Acta Cryst.*, **E67**, 952 (2011).

[27] M.I. Mohamadin, N. Abdullah, K.M. Lo, S.W. Ng. *Acta Cryst.*, **E66**, 1530 (2010).

[28] N. Abdullah, M.I. Mohamadin, S.W. Ng, E.R.T. Tiekink. *Z. Kristallogr.*, **227**, 122 (2012).

[29] L.N. Ozair, N. Abdullah, H. Khaledi, E.R. Tiekink. *Acta Cryst.*, **E66**, 589 (2010).

[30] M. Devereux, D. O'Shea, M. O'Connor, H. Grehan, G. Connor, M. McCann, G. Rosair, F. Lyng, A. Kellett, M. Walsh, D. Egan, B. Thati. *Polyhedron*, **26**, 4073 (2007).

[31] N. Abdullah, M.I. Mohamadin, A.P. Safwan, E.R. Tiekink. *Acta Cryst.*, **E66**, 1055 (2010).

[32] N.S. Ahmad Tajidi, N. Abdullah, Z. Arifin, K.W. Tan, S.W. Ng. *Acta Cryst.*, **E66**, 887 (2010).

[33] N.S. Ahmad Tajidi, N. Abdullah, Z. Arifin, K.W. Tan, S.W. Ng. *Acta Cryst.*, **E66**, 888 (2010).

[34] L.F. Lindoy, M.S. Mahinay, B.W. Skelton, A.H. White. *J. Coord. Chem.*, **56**, 1203 (2003).

[35] N.S. Ahmad Tajidi, N. Abdullah, Z. Arifin, K.W. Tan, S.W. Ng. *Acta Cryst.*, **E66**, 889 (2010).

[36] N.S. Ahmad Tajidi, N. Abdullah, Z. Arifin, K.W. Tan, S.W. Ng. *Acta Cryst.*, **E66**, 890 (2010).

[37] M.I. Mohamadin, N. Abdullah. *Cent. Eur. J. Chem.*, **8**, 1090 (2010).

[38] M.I. Mohamadin, N. Abdullah. *Int. J. Phys. Sci.*, **6**, 2526 (2011).

[39] G.M. Sheldrick. *SADABS, Program for Empirical Absorption Correction of Area Detector Data*, University of Göttingen, Göttingen (1996).

[40] Bruker. *APEX2 and SAINT*, Bruker AXS Inc., Madison, WI (2007).

[41] G.M. Sheldrick. *Acta Crystallogr., Sect. A: Found. Crystallogr.*, **64**, 112 (2008).

[42] C.S. Fountain, W.E. Hatfield. *Inorg. Chem.*, **4**, 1368 (1965).

[43] M. Kato, H.B. Jonassen, J.C. Fanning. *Chem. Rev.*, **64**, 99 (1964).

[44] G. Bain, J. Berry. *J. Chem. Educ.*, **85**, 532 (2008).

[45] J. Catterick, P. Thornton. *Adv. Inorg. Chem.*, **20**, 291 (1977).

[46] O. Kahn. *Molecular Magnetism*, VCH Publishers Inc., New York, NY (1993).

[47] D. Czakis-Sulikowska, A. Czylkowska. *J. Therm. Anal. Calorim.*, **71**, 395 (2003).

[48] A.J. Bard, L.R. Faulkner. *Electrochemical Methods: Fundamental and Applications.*, Wiley, New York, NY (2001).